How to construct log-Gabor Filters?

S. Fischer, R. Redondo and G. Cristóbal

Instituto de Optica (CSIC), Serrano 121, 28006 Madrid, Spain

July 5, 2009

1. Antecedents

Firstly proposed by Dennis Gabor in 1946 [1], the canonical coherent states of the Gabor filters are different versions of a Gaussian-shaped window shifted in time/space and frequency variables [2] [3], Gabor's work synthesizes the studies of Nyquist in Communication Theory in 1924 [4] and Heisenberg in Quantum Mechanics in 1927, by which he proposed the Gaussian shape as an optimal envelope for time-frequency representation turning the uncertainly principle from inequality into equality.

Some important characteristics of Gabor wavelets are [5]:
- Construction by a linear combination.
- Energy preservation in transform domain (Parseval's theorem).
- Non-orthogonality but an unconditional basis, a frame [6].
- Symmetry of the Fourier domain.
- Time/space and frequency shift-invariance.
- Localization: monomodal and isotropic.
- Regularity: smooth and infinitely derivable.

In the field of image processing another two characteristics arise:
- Directionality: filters can be rotated to discriminate spectral features in multiples directions (orthogonal wavelets have well-known difficulties to discriminate more than three orientations).
- Complex modulation (odd/even phases): effective for analyzing different phased features like abrupt ridges or edges.

Their widely usage in multiple fields can be taken as a prove of their success: texture analysis/synthesis [7, 8, 9], contour extraction [10, 11, 12, 13], segmentation [14], object recognition [15, 16, 17], image analysis and compression [18], movement estimation [19] or image restoration [20, 21].

2. Self-invertible log-Gabor filters

One step further, the recent filter design proposed by Sylvain Fischer [22] come to solve some of the traditional disadvantages that have complicated the functionality of Gabor filters. Log-Gabor filters basically consist in a logarithmic transformation of the Gabor domain [23] which eliminates the annoying DC-component allocated in medium and high-pass filters.
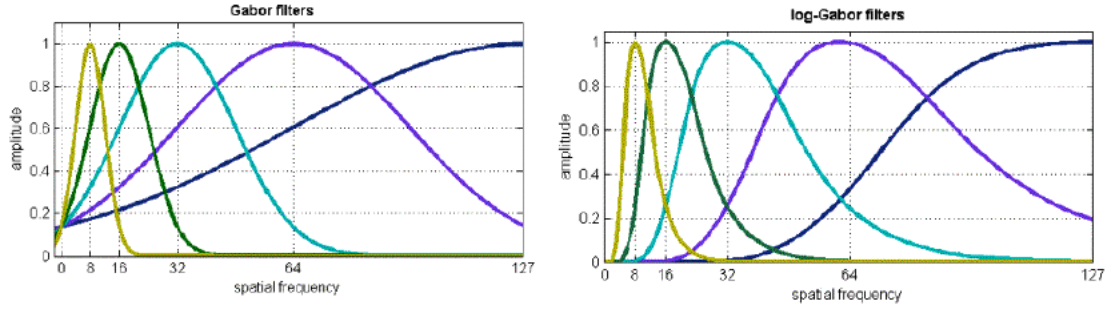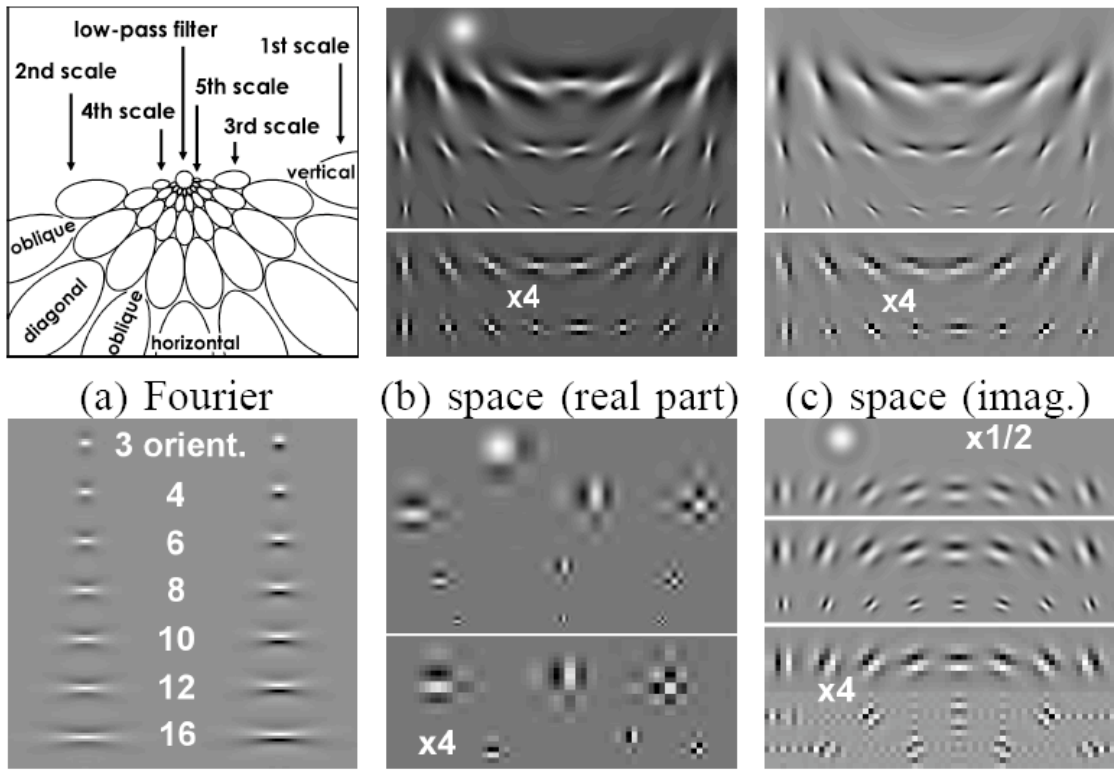
Fig. 1: Profiles of the frequency response of Gabor filters (left) and log-Gabor filters (right). Note that DC-component is minimized by the introduction of logarithms and the bands become more disjoined

(a) Fourier   (b) space (real part)   (c) space (imag.)

(d) log-Gabor   (e) 'Db4' wavelets   (f) Steerable pyramid

Fig. 2: Multiresolution schemes. **a.** Schematic contours of the log-Gabor filters in the Fourier domain with 5 scales and 8 orientations **b.** Real part in the spatial domain. **c.** Imaginary part in the spatial domain. **d.** In the proposed scheme the elongation of log-Gabor wavelets increases with the number of orientations (real parts in the left column and imaginary parts in the right column). **e.** Orthogonal wavelet filters 'Db4' for comparison. **f.** Steerable pyramid filters for comparison.

$$G_{pk} = G(\rho, \theta, p, k) = \exp\left(-\frac{1}{2}\left(\frac{\rho - \rho_k}{\sigma_\rho}\right)^2\right) \exp\left(-\frac{1}{2}\left(\frac{\theta - \theta_{pk}}{\sigma_\theta}\right)^2\right)$$

$$\text{with} \quad \begin{cases} \rho_k = \log_2(n) - k \\ \theta_{pk} = \begin{cases} \frac{\pi}{P}p & \text{if } k \text{ is odd} \\ \frac{\pi}{P}(p + \frac{1}{2}) & \text{if } k \text{ is even} \end{cases} \\ (\sigma_\rho, \sigma_\theta) = 0.996\left(\sqrt{\frac{2}{3}}, \frac{1}{\sqrt{2}}\frac{\pi}{P}\right) \end{cases}$$

in which (ρ, θ) are the log-polar coordinates (octave scales), k indexes the scale and p is the orientation, the pair $(\rho_k; \theta_{pk})$ corresponds to the frequency center of the filters, and $(\sigma_\rho; \sigma_\theta)$ the angular and radial bandwidths.

The main particularity of this novel scheme is the construction of the low-pass and high-pass filters [22]. Such a complete scheme approximates flat frequency response and therefore exact image reconstruction which is obviously beneficial for applications in which inverse transform is demanded, such as texture synthesis, image restoration, image fusion or image compression.

A. Low pass filter

It could be defined simply as a Gaussian low-pass filter as in [8]. Nevertheless for a better filling-in of the residual low, two additional scales above the number of scales are built and summed up together (as the root sum squared). Moreover the part inside the highest additional scale is set up to one. In practice if 5 scales are deployed, the filters that would correspond to the 6th and 7th scales are summed and additionally the space inside the 7th scale ($\rho < \log_2 n - 7$) is set up to one (see the upper left part Fig. 2.a).

B. High-pass filters

The first scale present a significant amplitude above the Nyquist frequency ($\rho \geq \log_2(n/2)$). If it is cut off abruptly the filter shape is severely distorted in the spatial domain. For this reason many implementations avoid to cover such high frequency range. One alternative consists in a non-oriented high-pass filter [3], nevertheless it can introduce cross-shaped artifacts. The solutions proposed by Sylvain Fischer consist in incorporating first a half-pixel shifting in the spatial position of the imaginary part of the filters. This shift allows the first scale filters to capture much more adequately the antisymmetric features.

B.1 Real part of the horizontal and vertical filters: defined by central symmetry, they are continuous across the periodicities of the Fourier domain which is important since strong discontinuities in the Fourier domain create side lobes and a worst localization in the spatial domain. They are also well localized, without extra side lobes in the spatial domain (see Fig. 2 and Fig. 3).
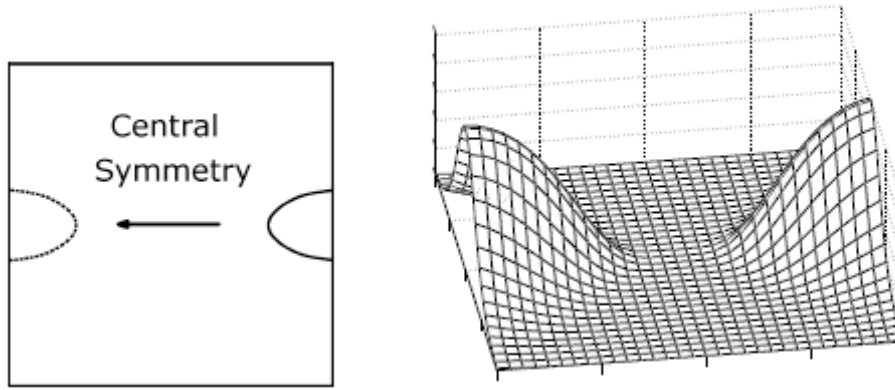
Fig. 3: Real part of high-pass filter.

B.2 Real part of oblique filters: defined by central symmetry. To maintain the Fourier domain continuous (across periods) and to keep a good localization in the space domain they are fold up by considering a periodicity of order n. To maintain the filter selectivity to high-frequencies, it is then necessary to filter down the induced lowest frequencies by multiplying the folded part by an attenuation factor α defined here as a raised cosine function (see Fig. 4).

(a) oversampled filter   (b) folding   (c) α

(d) attenuation   (e) symmetry
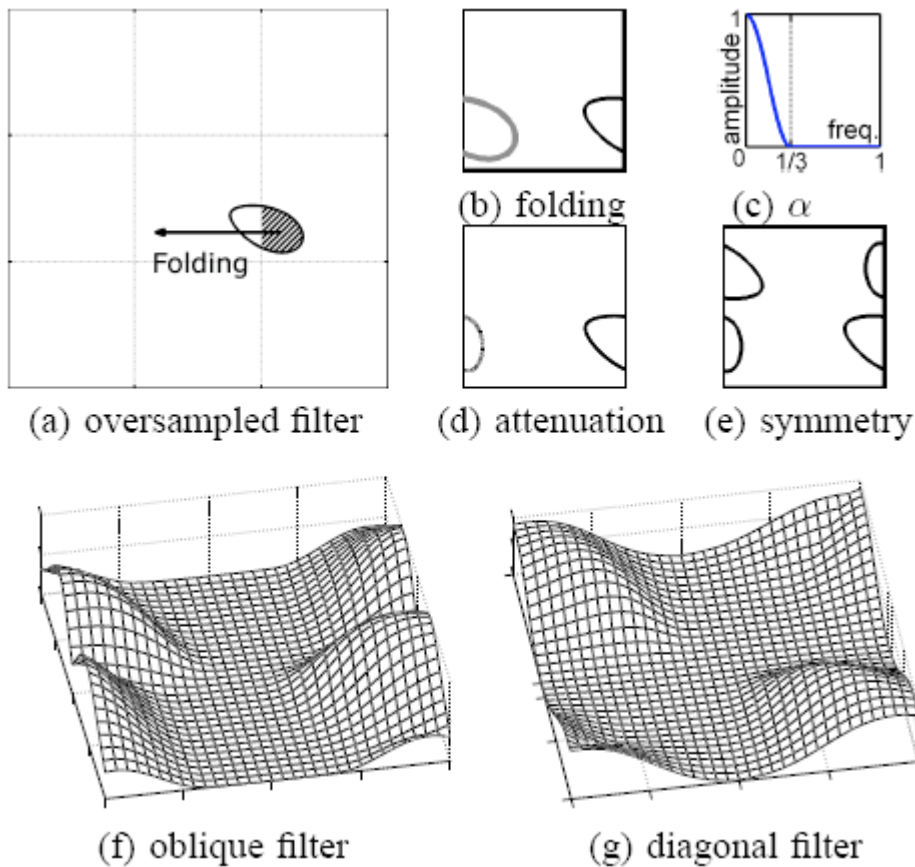
(f) oblique filter   (g) diagonal filter

Fig. 4: Real part of oblique first scale filters in the Fourier domain. **a.** The frequency domain is oversampled 3 times. **b.** The frequencies above the Nyquist frequency are folded up by periodicity. **c.** Raised cosine function. **d.** The folded part of the filter is multiplied by the

raised cosine function. **e.** The central symmetry is summed up for the construction
of a real-valued filter. **f.** Resulting oblique filter. **g.** Resulting diagonal filter.

B.3 Imaginary part of the horizontal and vertical filters: in the spatial domain the
imaginary part have to be antisymmetric, but here the axis of central antisymmetry will
not be localized in a pixel but in between two pixels. The first justification is that an
antisymmetric filter would have a zero as central coefficient in the spatial domain. The
filter would then be very coarsely localized, having most of its amplitude far from its
center (see Fig. 5.a). The second reason is that an antisymmetric high-pass filter is not
continuous across periods in the Fourier domain, while a half-pixel shifted version
do is (see Fig. 5.b). The half pixel displacement is induced by multiplying $e^{i\pi}$ un or $e^{i\pi}$
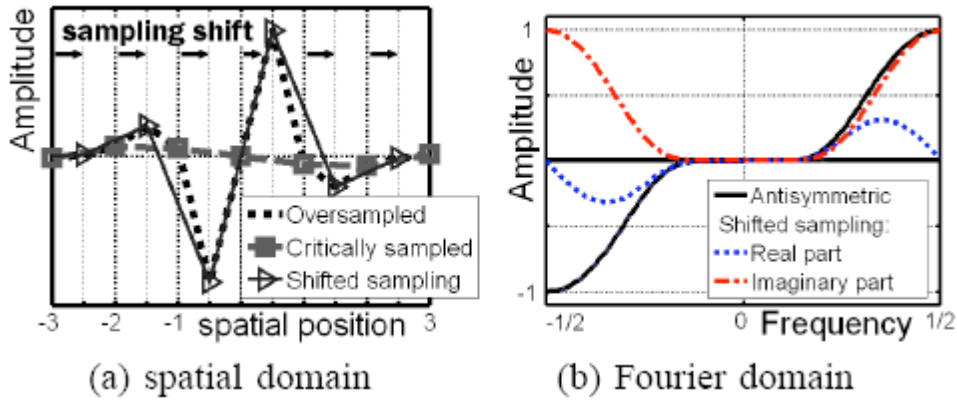

(a) spatial domain   (b) Fourier domain

Fig. 5: Imaginary part of horizontal and vertical high-pass filters. **a.** Pixel shifting in the
spatial domain compared to a non-shifted version and a oversampled version. **b.**
Shifting produces complex-valued coefficients in the Fourier domain and it makes the
filter continuous in its frequency coverage across periods.

B.4 Imaginary part of oblique filters: they are defined antisymmetrically with the same
attenuation function α and also shifted half-pixel perpendicularly to the preferred
direction of the filter by multiplying $e^{\frac{i\pi}{n}(u \cdot t_u + v \cdot t_v) \cdot max(|t_u|,|t_v|)}$ where $(t_u,$
$t_v)$ is the normalized vector of the preferred filter direction.

B.5 Second scale filters: defined with periodicity and attenuation α but here
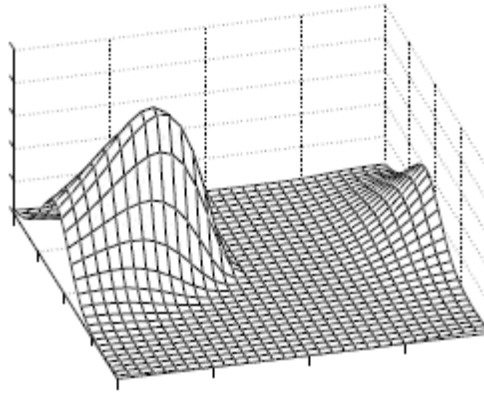the half-pixel shifting it is not necessary (Fig. 6).

Fig. 6: Second scale filters constructed in the Fourier domain by folding the filters by periodicity and applying the attenuation function on the folded part.

Note that, because the definition of the first scale filters differs from the other scales, the transform is no more strictly a "wavelet" one, but it can be considered as a wavelet-like transform since the general shape of the basis functions is obtained by translation, dilatation, and rotation of a mother function if we except the modifications proposed here for improving the reconstruction performance.

Note also that this log-Gabor implementation is non-orthogonal, which implies a considerable increasing of computational and memory costs. However overcompleteness entails important benefits in terms of analysis and image quality reconstruction.

3. Overcompleteness

In order to achieve (bi-)orthogonality, wavelets are critically sampled which besides implies reducing time consumption and memory storage. Recent works, however, have claimed the necessity for using overcomplete
representations to solve not few drawbacks shown by (bi-)orthogonal wavelets,
namely lack of shift-invariance (shiftability), aliasing between bands, poor resolution in orientation and insufficient match with image features [24, 25, 26, 27]. In spite of exact reconstruction, in applications where the wavelet coefficients have to be manipulated, the aliasing created by filter overlapping becomes often visible as distortion.

The relaxation of the critical subsampling necessarily implies overcompleteness, which means that the number of vectors to the transformed space is larger than those required to complete a basis. That sampling relaxation allows to design filters with interesting properties such as shift-invariance and reduced aliasing effects [24].
Overcomplete basis have already shown more efficiency in restoration [28, 29, 30], and other like the steerable pyramid [31, 24], contourlets [25] or curvelets [33] have been proposed to ameliorate orientation sensitivity, benefiting contour detection and noise removal.

As in the case of Gabor filters, a special interest is growing during last years in overcomplete complex wavelets. These wavelets are composed of paired filters

(real/imaginary) in opposite/quadrature phase, which are able to provide simultaneously local maxima independently whether the featured signal is odd or even, as for example edges and ridges respectively. Complex wavelets have been proposed for image compression [34, 35], texture analysis [36, 37] and recently for image fusion [38, 39, 40,41].

4. References

[1] D. Gabor. Theory of Communication. J. Inst. Electr. Eng., 93:429 457, 1946.

[2] L. Cohen. Generalized phase-space distribution functions. J. Math. Phys., 7:781_786, 1966.

[3] J. Morlet, G. Arens, E. Fourgeau, and D. Girard. Wave propagation and sampling theory. Geophysics, 47:203_236, 1982.

[4] H. Nyquist. Certain factors affecting telegraph speed. Bell Systems Technical Journal, 3:324, 1924.

[5] J.K. Kamarainen, V. Kyrki, and H. Kälviäinen. Invariance properties of Gabor filter based features - overview and applications. IEEE Transactions on Image Processing, 15(5):1088_1099, 2006.

[6] I. Daubechies. Ten lectures on wavelets. SIAM, Philadelphia, PA, 1992.

[7] M. Bovik, A.C. Clark and W.S. Geisler. Multichannel texture analysis using localized

spatial _lters. IEEE Trans. Pattern Analysis Machine Intelligence, 12(1):55_73, 1990.

[8] J. Portilla, R. Navarro, O. Nestares, and A. Tabernero. Texture synthesis-by-analysis based on a multiscale early-vision model. Opt. Eng., 35(8):1_15, 1996.

[9] Y.M. Ro, M. Kim, H.K. Kang, B.S. Manjunath, and J. Kim. MPEG-7 homogeneous texture descriptor. ETRI Journal, 23(2):41_51, 2001.

[10] F. Heitger, L. Rosenthaler, R. Heydt, E. Peterhans, and O. Kubler. Simulation of neural contour mechanisms: from simple to end-stopped cells. Vision Research, 5(5):963_981,1992.

[11] L. Rosenthaler, F. Heitger, O. Kübler, and R. von der Heydt. Detection of general edges and keypoints. In European Conference on Computer Vision, pages 78_86, 1992.

[12] P. Kovesi. Image features from phase congruency. J. Comput. Vis. Res., 1(3):2_27, 1999.

[13] C. Grigorescu, N. Petkov, and M. A. Westenberg. Contour detection based on nonclassical receptive field inhibition. IEEE Trans. on Image Proc., 12(7):729_739, 2003.

[14] J.V.B. Soares, J.J.G. Leandro, R.M.C. Jr, H.F. Jelinek, and M.J. Cree. Retinal vessel segmentation using the 2-D Gabor wavelet and supervised classification. IEEE Trans. on Medical Imaging, 25(9):1214_1222, 2006.

[15] M. Pötzsch, N. Krüger, and C. Malsburg. Improving object recognition by transforming Gabor filter responses. Network: Computation in Neural Systems, 7(2):341_347, 1996.

[16] N. Krüger, M. Pötzsch, and G. Peters. Principles of cortical processing applied to and motivated by artificial object recognition. In P. Hancock R. Baddeley and P. Foldiak, editors, Information Theory and the Brain, pages 223_228. Cambridge University Press, 1998.

[17] V. Krüger. Gabor wavelet networks for object representation. PhD thesis, Christian- Albrechts-University Kiel, Technical Faculty, 2001.

[18] J. Daugman. Complete discrete 2-D Gabor transforms by neural networks for image analysis and compression. IEEE Trans. Acoust. Speech Signal Proc., 36(7):1169_1179, 1988.

[19] D.J. Heeger. Model for extraction of image flow. J. Opt. Soc. Amer. A, 4(8):1455_1471, 1987.

[20] I. Daubechies. Orthonormal bases of compactly supported wavelets. Comm. Pure Applied Math., XLI(41):909_996, 1988.

[21] P. Kovesi. Phase preserving denoising of images. In Australian Pattern Recog. Soc. Conf. DICTA'99. Perth WA., pages 212_217, 1999.

[22] S. Fischer, F. Sroubek, L. Perrinet, R. Redondo, and G. Cristóbal. "Self-invertible log-Gabor wavelets". Int. Journal of Computer Vision, 75 (2), p. 231-246, 2007.

[23] D.J. Field. Relation between the statistics of natural images and the response properties of cortical cells. J. Opt. Soc. Am. A, 4(12):2379_2394, 1987.

[24] E.P. Simoncelli, W.T. Freeman, E.H. Adelson, and D. J. Heeger. Shiftable multiscale transforms. IEEE Trans. Inf. Theory, 38(2):587_607, 1992.

[25] M. Do and M. Vetterli. The contourlet transform: An efficient directional multiresolution image representation. IEEE Trans. on Image Proc., 14(12):2091_2106, 2005.

[26] N.G. Kingsbury. Complex wavelets for shift invariant analysis and filtering of signals.
Jour. of Applied and Comput. Harmonic Analysis, 10(3):234_253, 2001.

[27] D. Donoho and A.G. Flesia. Can recent innovations in harmonic analysis 'explain' key findings in natural image statistics. Computation in Neural Systems, 12(3):371_393, 2001.

[28] R.R. Coifman and D. Donoho. Translation-invariant de-noising. In A. Antoniadis and G. Oppenheim, editors, Wavelets and statistics, Lecture Notes in Statistics 103, pages 125_150. Springer Verlag, New York, NY, 1995.

[29] X. Li and M.T. Orchard. Spatially adaptive image denoising under overcomplete expansion. In IEEE Int. Conf. on Image Proc., volume 3, pages 300_303, 2000.

[30] Yung-Ching Chang, Bin-Kai Shyu, Chuan-Yu Cho, and Jia-ShungWang. Adaptive postprocessing for region-based fractal image compression. In Data Compression Conference, page 549, 2000.

[31] W.T. Freeman and E.H. Adelson. The design and use of steerable filters. IEEE Trans. Pattern Analysis Mach. Intell, 13(9):891_906, 1991.

[33] J. L. Starck, E. J. Candés, and D. L. Donoho. The curvelet transform for image denoising. IEEE Trans. on Image Proc., 11(6):670_684, 2002.

[34] W. Lawton. Applications of complex valued wavelet transforms to subband decomposition. IEEE Trans. Signal Processing, 41:3566_3568, 1993.

[35] N.G. Kingsbury. Complex wavelets for shift invariant analysis and filtering of signals. Jour. of Applied and Comput. Harmonic Analysis, 10(3):234_253, 2001.

[36] M.H. Gross and R. Koch. Visualization of multidimensional shape and texture features in laser range data using complex-valued Gabor wavelets. IEEE Trans. Visual. And Comput. Graphics, 1(1):44_59, 1995.

[37] J. Portilla, R. Navarro, O. Nestares, and A. Tabernero. Texture synthesis-by-analysis based on a multiscale early-vision model. Opt. Eng., 35(8):1_15, 1996.

[38] P. Hill, N. Canagarajah, and D. Bull. Image fusion using complex wavelets. In BMVC, 2002.

[39] B. Forster, D. Van De Ville, J. Berent, D. Sage, and M. Unser. Complex wavelets for extended depth-of-_eld: A new method for the fusion of multichannel microscopy images. Microscopy Research and Technique, 65(1-2):33_42, September 2004.

[40] J.J. Lewis, R.J. O'Callaghan, S.G. Nikolov, D.R. Bull, and C.N. Canagarajah. Regionbased image fusion using complex wavelets. In Proc. of the 7th Int. Conf. on Information Fusion, pages 555_562, 2004.

[41] R. Redondo, F. Sroubek, S. Fischer and G. Cristóbal. "Multifocus image fusion using log-Gabor wavelets and a multisize windows technique". *Journal of Information Fusion*, 10 (2), p. 163-171, 2009.

[42] W. Sweldens. The lifting scheme: A construction of second generation wavelets. Siam J. Math, 29(2):511_546, 1997.

[43] N. Ranganathan, R. Mehrotra, and K. Namuduri. An architecture to implement multiresolution. In Proceedings of the International Conference on Acoustics, Speech, and Signal Processing, volume 2, pages 1157_1160, 1991.

[44] O. Nestares, R. Navarro, J. Portilla, and A. Tabernero. Effcient spatial-domain implementation of a multiscale image representation based on Gabor functions. Jour. of Eletr. Imag., 7(1):166_173, 1998.

[45] J. Ilonen, J.K. Kamarainen, and H.K Kälviäinen. Efficient computation of Gabor features. Technical Report 100, Department of Information Technology, Lappeenranta University of Technology, 2005.

[46] S. Mallat and Z. Zhang. Matching pursuits with time-frequency dictionaries. IEEE Trans. on Signal Proc., 41(12):3397_3415, 1993.

[47] S.S. Chen, D.L. Donoho, and M.A. Saunders. Atomic decomposition by basis pursuit. SIAM Jour. on Sc. Computing, 20(1):33_61, 1999.

[48] L. Perrinet, M. Samuelides, and S. Thorpe. Coding static natural images using spiking event times: do neurons cooperate? IEEE Trans. on Neural Networks, 15(5):1164_1175, 2004.

[49] S. Fischer, G. Cristóbal, and R. Redondo. Sparse overcomplete Gabor wavelet representation based on local competitions. IEEE Trans. on Image Proc., 15(2):265_272, 2006.